ADC-based real-time signal processing for the PANDA Straw Tube Tracker

L. Jokhovets, M. Drochner, A. Erven, W. Erven, G. Kemmerling, H. Kleines, P. Kulessa, H.W. Loevenich, P. Marciniewski, M. Mertens, H. Ohm, K. Pysz, J. Ritman, V. Serdyuk, S. v. Waasen, P. Wintz, P. Wüstner

***Abstract*–The PANDA (AntiProton Annihilations at Darmstadt) experiment is being built at the new Facility for Antiproton and Ion Research (FAIR) in Darmstadt Germany. PANDA will measure antiproton-proton annihilation reactions in the charm quark mass range to investigate the nature of the strong interaction. This particle physics experiment will run at very high reaction rates of 10- 20 MHz.**

Our work is related to an ADC (analog-to-digital converter) based data acquisition system for the PANDA Straw Tube Tracker (STT). The STT will be able to deliver data rates up to 20 GByte/s through over 4600 signal channels and could require major efforts for the hardware implementation as well as high offline processing power.

Test beam studies were carried out in order to specify a proper system architecture with feasible hardware and to reduce output data stream to a level suitable for offline processing.

We analyze the straw tube response to both the proton beam and ^{55}Fe irradiation. Furthermore, we present real-time processing using the neighboring straw information and introduce the technique to reconstruct the tracks.

***Index Terms*-data acquisition, digital signal processing, particle tracking.**

I. Introduction

The PANDA (AntiProton Annihilations at Darmstadt) experiment at FAIR (Facility for Antiproton and Ion Research) investigates antiproton-proton annihilations and the nature of the strong interaction. The Straw Tube Tracker (STT) is the main tracking detector for charged particles in the PANDA target spectrometer. It consists of 4636 single straw tubes, arranged in a large cylindrical volume around the beam-target interaction point (Fig. 1).

The STT is designed for:

- spatial reconstruction of the helical trajectories of charged particles in a broad momentum range from a few 100 MeV/c up to 8 GeV/c,
- measurement of the particle momentum by the reconstructed trajectory in the solenoidal magnetic field,
- and measurement of the specific energy loss (dE/dx) for particle identification to separate protons, kaons and pions in the momentum region up to about 1 GeV/c [1].

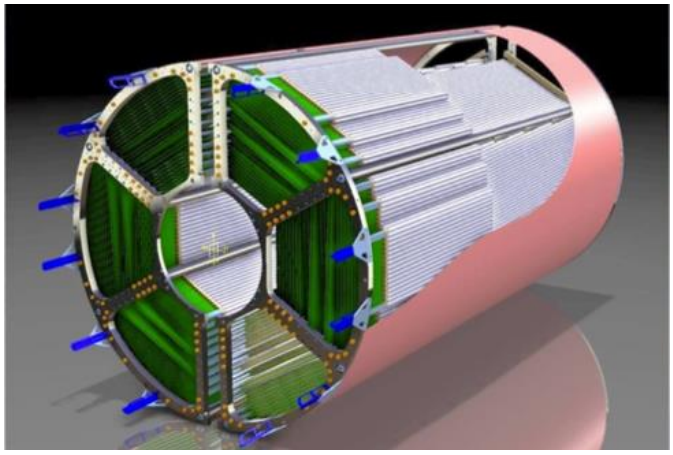

Fig. 1. Artistic view of the PANDA straw tube tracker.

In this work we focus on the particle track reconstruction, which is the most critical task among those mentioned above. To determine the track position in drift chambers, the arrival time of ionization electrons is measured with an analog-to-digital converter (ADC) based method. According to this method, the signal shape is sampled at a constant rate, providing multiple points per signal for the extraction of time information. Calculation of the electron arrival time is performed in field programmable gate arrays (FPGAs). The back-end system collects the information from FPGA channels, provides clustering and reconstructs the track.

The STT data acquisition (DAQ) system has a large number of processing channels, one for each of the 4636 straw tubes. A high particle rate (up to about 1 MHz per straw tube) will result in a high data rate (up to 20 GByte/s) delivered to the back-end system for offline processing. Such a system requires major efforts for the hardware implementation as well as high offline processing power and storage capability.

We start with an analysis of a single pulse produced by an ^{55}Fe source in order to determine the optimal combination of shaping time and sampling rate (Section II). Our motivation is to minimize the required digitization and real-time processing

Manuscript received May 09 2014

L. Jokhovets, M. Drochner, A. Erven, W. Erven, G. Kemmerling, H. W. Loevenich, H. Kleines, M. Mertens, H. Ohm, T. Preuhs, J. Ritman, V. Serdyuk, S. v. Waasen, P. Wintz, P. Wüstner are with Forschungszentrum Jülich, Wilhelm-Johnen-Strasse, 52428 Jülich, Germany (telephone: +49 2461 614569, e-mail: l.jokhovets@fz-juelich.de).

P. Kulessa, K. Pysz are with Institute of Nuclear Physics PAN, ul. Radzikowskiego 152, 31-342 Krakow, Poland

P. Marciniewski is with Uppsala University, Uppsala, Sweden

power. Then, aiming to reduce the data rate to a level suitable for offline processing, we investigate the proton beam response (Section III) and introduce real-time processing dependent on the neighboring straw data (Section IV). This processing is implemented in FPGAs and includes event building and filtering, self-triggering and clustering, and multiple track resolution.

An ADC-based method allows us to see details (due to pulse shape analysis), whereas real-time processing depending on the neighboring channels data allows the system to be considered as a whole by choosing the interpretation of the details, making the decision about its relevance and rejecting the irrelevant data.

II. Shaping Time, Sampling Rate and Time Resolution

A. Measuring setup and methodology used in tests

In our experiments we use the data acquisition system originally developed for the WASA at COSY experiment [2], [3]. The straw tube readout chain consists of a front-end transimpedance amplifier followed by a second-order low-pass filter with a time constant of 3 ns. This is followed by a flash analog-to-digital converter (FADC) with a sampling rate of 240 MHz, and the FPGA processing unit, which determines the leading edge time and energy loss features via pulse shape analysis.

The digitized data are buffered continuously in the FPGA random access memory built as a ring buffer. Processing of these data is trigger-initiated. The acquisition modules can also be programmed to record the raw sampled data for investigation purposes.

For the extraction of the leading edge time, a constant fraction discriminator (CFD) technique has been exploited. The technique uses a threshold which is set to a certain fraction of the signal peak. This fraction was 0.5 in our experiments. To achieve a time resolution better than 4.17 ns (the sampling interval corresponding to a sampling rate of 240 MHz), a linear interpolation of the rising edge through the two sampling points closest to the threshold has been carried out (as shown in the right part of Fig. 2). The calculations are performed in the FPGA with a discretization of 1/16 of the sampling interval. This leads to a time binning of 260 ps in our measurements.

In order to explore data from multiple straw tubes simultaneously, we have modified this system by introducing the real-time processing feature. Furthermore, the system can run at the original sampling rate of 240 MHz as well as at the reduced rate of 120 MHz, involving only every second sample into the processing. The modified system is used in our experiments.

B. Single cluster response to ^{55}Fe irradiation

The primary cluster energy by irradiation with an ^{55}Fe source is 5.9 and 2.9 keV. At the formation, the spatial extension of an ionization cluster is small, usually less than 100 µm. At the end of the drift length, the spatial distribution of the electrons is Gaussian with characteristic longitudinal and transverse widths. The spread of the arrival times is given by the longitudinal width and the drift velocity [4]. Assuming a standard deviation of the spatial diffusion (spread of the charge distribution along the drift direction) of about 200 µm for 1 cm of drift and an electron drift velocity of 50 µm/ns, we get a cluster pulse duration of about 3-4 ns for primary ionization near the wire and of about 5-6 ns for primary ionization near the wall.

Fig. 2 shows the response to ^{55}Fe irradiation sampled at 240 MHz using Ar/CO_2(90/10) gas mixture. The data points are the average of 60,000 straw tube responses. The pulse duration is 28-40 ns.

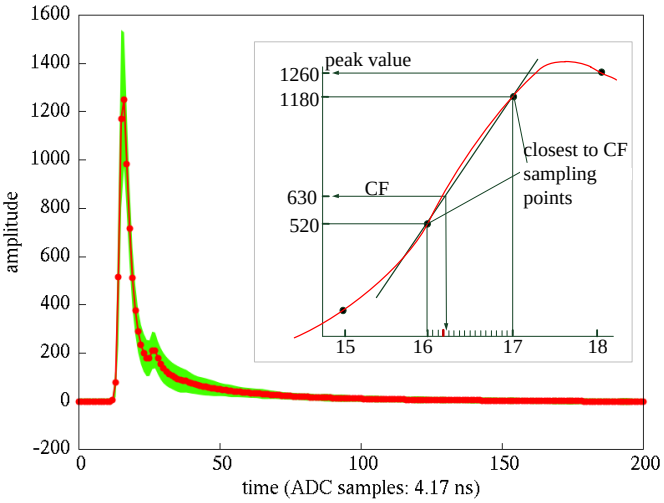

Fig. 2. Sampled response to ^{55}Fe irradiation. The solid line shows the mean value averaged over 60,000 responses, while the shaded band indicates the standard deviation. The inset illustrates the constant fraction method with linear interpolation of the rising edge through the two sampling points closest to the threshold value denoted by CF.

The difference between the estimated and measured values can be explained by the electronic channel unipolar shaping (second-order low-pass filter with time constant of 3 ns). Note that the sampling rate can be optimized by changing the time constant.

C. Single cluster response to a beam of protons

The average energy loss at atmospheric pressure for minimum ionizing particles in argon gas is 2.44 keV/cm and the number of primary ion pairs is about 29.4 per cm [5]. This means that the energy of most primary clusters is ~83 eV, i.e. at least 30 times lower than for primary clusters from an ^{55}Fe source. Such a signal with an amplitude of 40-50 ADC units is comparable to the system noise level (of approximately 40 units). As a result, in our experiments we only register a fraction of ionization clusters, which have a higher primary energy than the average one. Not only are those clusters registered with an above-average primary energy, but some low-energy clusters are also registered due to overlap with others.

D. Sampling rate and shaping time

We aim to reduce the sampling rate, and thus to

- minimize digitization and FPGA processing efforts

• increase the integration level by processing a larger number of channels within a single FPGA.

The first point involves reducing of the hardware implementation efforts, and the second facilitates accessing information from neighboring channels during the real-time processing of the data.

In order to obtain the required precision for the track reconstruction, a total system time resolution of better than 1 ns must be achieved [1]. As mentioned above, the 240 MHz sampling system (currently used) provides a binning of 260 ps utilizing the CFD technique. We estimate that the highest uncertainty in the peak value measurement also contributes ~ 260 ps and appears when the pulse peak occurs between two neighboring samples with approximately equal amplitudes. A possible nonlinearity of the pulse rising edge gives an additional uncertainty of less than 80 ps. Thus, the total measurement error is less than 600 ps and fulfills the above-mentioned requirements. This makes this setup suitable as a reference for further comparison with a lower sampling rate configuration. In the 120 MHz setup, linear interpolation with binning of 260 ps was also used. The sampling rate comparison tests with ^{55}Fe irradiation over the 60,000 measurements were completed. For each measurement, the constant fraction time was determined with 120 and 240 Msps (mega samples per second). Then, the difference between the times determined with 120 and 240 Msps was calculated in units of bins (260 ps). The distribution of the time difference is shown in Fig. 3.

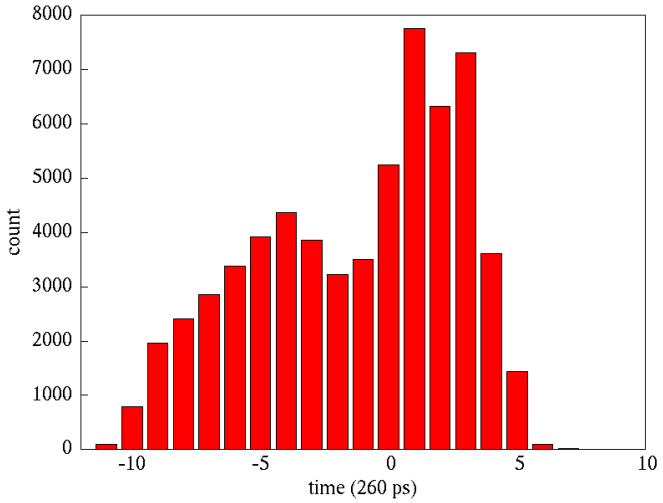

Fig. 3. Distribution of differences (in bins of 260 ps) between the constant fraction times measured with the sampling rates of 120 MHz and 240 MHz for ^{55}Fe irradiation. The root mean square (RMS) value of the distribution is 1.04 ns.

The root mean square (RMS) value of the distribution is 1.04 ns. Therefore the initial shaping time is not suitable for measurements with a low sampling rate of 120 MHz.

To improve the results, the shaping time was increased by increasing the length of the thin coax cable connecting the straw tube with the input amplifier (from 3 to 20 m). This led to an extension of the pulse duration and lowering of its amplitude. The deviation between measurements with 120 and 240 MHz appeared smaller (Fig. 5), and reached 300 ps using the signal fitting for the correction of the peak value done for 120 MHz processing (Fig. 6). The pulse response to ^{55}Fe irradiation with a duration of 80 ns was applied as a fitting curve. This curve does not completely match the pulse responses with another duration, as shown in inlays of Fig. 6. An improvement is required by adjusting the fitting curve to the duration of the straw tube pulse.

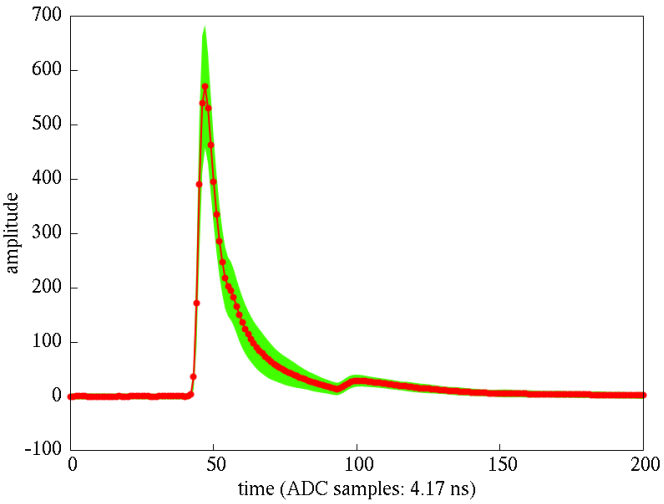

Fig. 4. Sampled response to ^{55}Fe irradiation using an increased shaping time due to cabling. The solid line shows the mean value, while the shaded band indicates the standard deviation. A small second peak is related to signal reflection at the amplifier, which is located at the end of 20 m cable.

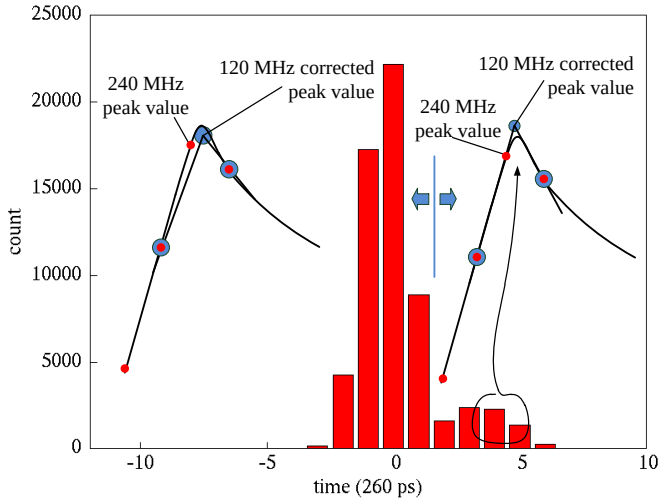

Fig. 5. Experiment with an increased shaping time. Distribution of differences (in bins of 260 ps) between the constant fraction (CF) times measured with the sampling rates of 120 MHz (first setup) and 240 MHz (second setup). The root mean square (RMS) value of the distribution is 0.42 ns. Due to the larger sampling time interval, the peak values of the 120 MHz setup are less than or equal to those values measured with the 240 MHz setup. Consequently, the CF obtained with the first setup is less than or equal to the CF of the second setup, which leads to the increased contribution of the negative values in the histogram (left part). The contribution of positive values appears only due to nonlinearity and discretization error (right part).

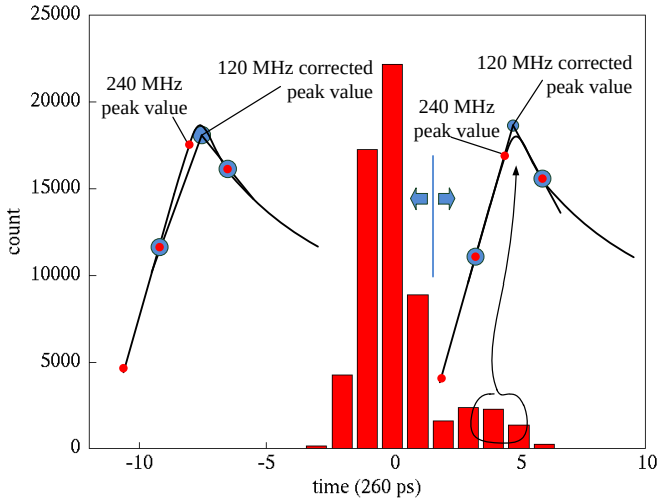

Fig. 6. Experiment with an increased shaping time. Distribution of differences between the constant fraction times measured with the sampling rates of 120 MHz and signal fitting for the correction of the peak value (first setup) and 240 MHz (reference setup). Due to the correction of the peak values, the first setup can deliver better results than the reference setup. In contrast to Fig. 5, the contribution of the negative value becomes smaller. It is related to discretization and nonlinearity errors. The contribution of the positive values is affected by fitting. It takes place by the erroneously high corrected peak value (seen in the right part of the fig.), while the fitting curve is not adjusted yet to the pulse width. The RMS of the distribution is 0.41 ns and 0.26 ns respectively with and without the contribution due to non-optimized fitting.

By increasing the shaping time, we increase the pulse duration and thus can reduce the sampling rate down to 120 MHz. In this case, single clusters with an above-average ionization energy as well as multiple clusters will be registered with about 300 ps loss of accuracy compared to the measurements at 240 MHz.

The question is how far we can increase the shaping time while reducing the sampling rate.

By reducing the sampling rate, we reduce the number of sampling points belonging to the native leading edge of the very first cluster (belonging to the front part of the summed response, where the very first cluster arrived at the wire is still not overlapped with another clusters arriving later). In order to get a response from the very first primary cluster and thus a better time resolution, a very high sampling rate should be used. Indeed, if the time between arriving clusters is 3 ns (case near the wire), the sampling rate should be around 600 MHz to get at least two samples on the native leading edge. Assuming the time between arriving clusters to be 0.3 ns (case of track near the wall), the sampling rate should be 6 GHz. This high sampling rate is inappropriate for the large-scale PANDA hardware. Moreover, considering the signal-to-noise ratio (SNR) of the currently used setup, a higher sampling rate does not improve the performance significantly because the first cluster signals are below the noise level.

Since it is not evaluated which SNR will be achieved at the PANDA experiment, we exploit the experience of other tracker experiments. We pick the Transition Radiation Tracker (TRT) in CERN ATLAS detector. To be safely over the noise, the low–threshold discriminator level is set to a level of 200-250 eV [6], [7]. Assuming the energy of most primary clusters to be ~83 eV, the time-to-wire distance will be calculated based on the summed response of the first 3 clusters. Compared to our currently used test setup, the SNR appears nearly the same. Moreover, taking a cluster spread from a track near the wire (the most critical path) of ~3 ns and a sampling rate of 120 MHz, we get 2 sampling points during the arrival of 3 clusters. Thus, the calculation of the track-to-wire distance is based on summed response of the same number of clusters for both setups.

It is estimated that the binning used in the TRT (~ 3 ns) contributes 0.042 mm to the overall spatial resolution (0.132 mm) of the tracker [8]. This parameter has a lower value of 600 ps in our experiment. Assuming an additional performance loss of ~300 ps when using interpolation instead of raising the sampling rate, the resolution in the system being developed should still be better than achieved for the ATLAS TRT.

III. Analysis of Proton Beam Test Measurements

In this section we consider in detail the system response to a beam of protons as a foundation for processing operations which will be introduced later.

The results discussed below were obtained with a beam of protons at 2.7 GeV/c, provided by COSY [9]. A gas mixture consisting of Ar/CO_2 with a mixing ratio of 90/10 and high voltage of 1800 V were used. Signals from 64 straw tubes in a test setup were sampled with 240 MHz and recorded in 5 μs time windows. The trigger for the readout was generated by an external scintillator detector.

An example of the response to multiple particle tracks crossing a straw tube by proton beam irradiation is shown in Fig. 7.

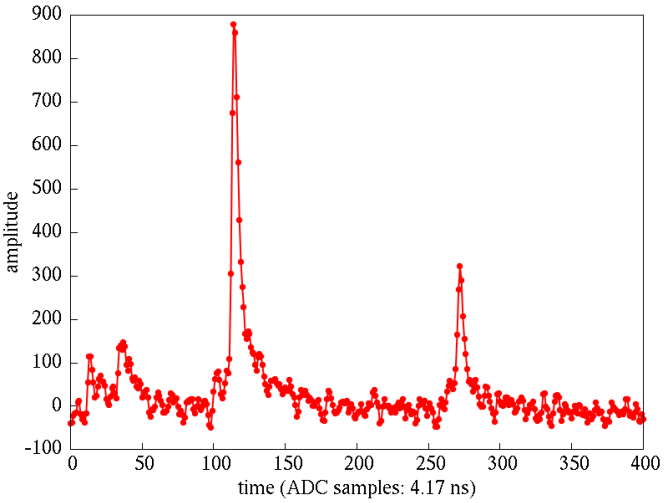

Fig. 7. Response to multiple particle tracks crossing a straw tube by proton beam irradiation.

A. *Pulse response interpretation*

Fig. 8 shows pulse responses of four straw tubes to the same particle track. The following features are of importance:

- For each straw tube, the leading edge gives the time of the first cluster arrived at the wire in each straw tube.

- The trailing edges have the same time for all straw tubes on the track.

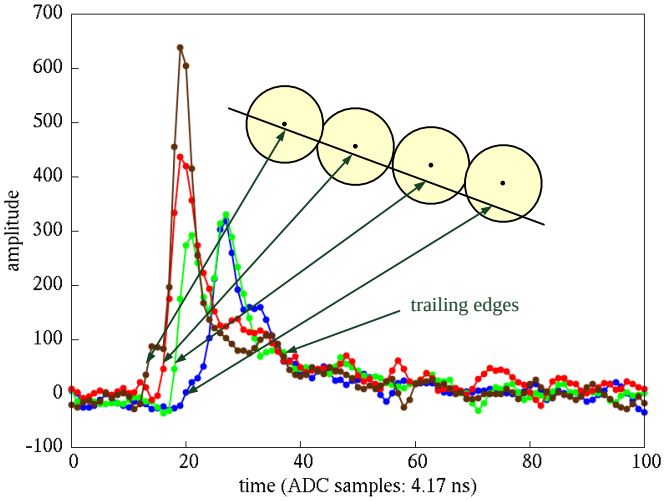

Fig. 8. Responses of four straw tubes to the same particle track.

- The pulse shape appears as a superposition of multiple cluster responses. This increases the number of sampling points in the leading edge compared to ^{55}Fe response (compare Fig. 2 and Fig. 8) and flattens the peaks of single cluster responses. When the particle track passes close to the wire, clusters arrive at the wire dispersed in time, and the pulse shape structure appears irregular. For the tracks passing far from the wire, the difference between the arrival times of clusters is on average smaller and the pulse shape is more regular.
- The signal width depends on the track position inside the straw: it is larger for a track passing close to the wire and narrower when a track crosses the straw tube close to the cathode (wall).

The best time resolution can be achieved with a shaping time close to zero. In this case, all cluster pulses are resolved as single peaks. The first maximum provides the arrival time of the first cluster while the maximum of the last pulse will determine the wall position. The combination of both parameters defines the track-to-wire distance. We estimate the discriminator technique parameters in terms of the smallest deviation from this case.

B. Particle tracks near the wire

If particles pass close to the wire, the clusters arrive at the wire dispersed in time, on average every 3 ns. Therefore, the superposed pulse has a relatively low amplitude and an irregular structure (Fig. 8, Fig. 10). In this case, the leading edge is formed by the overlap of 2-3 cluster responses and the native maximum of the first cluster to arrive overlaps with the later clusters.

If there are multiple inflection points on the leading edge (curves 1 and 2 in Fig. 9), the leading edge discriminator technique can give erroneously high time values, for example t_1 instead of t_0 as shown in Fig. 9. To deduce the information about the first cluster, the leading edge discriminator technique should only take the first few sampling points into account, as proven by the response to ^{55}Fe irradiation under defined conditions. In our case, this number is about 3-4 (Fig. 9).

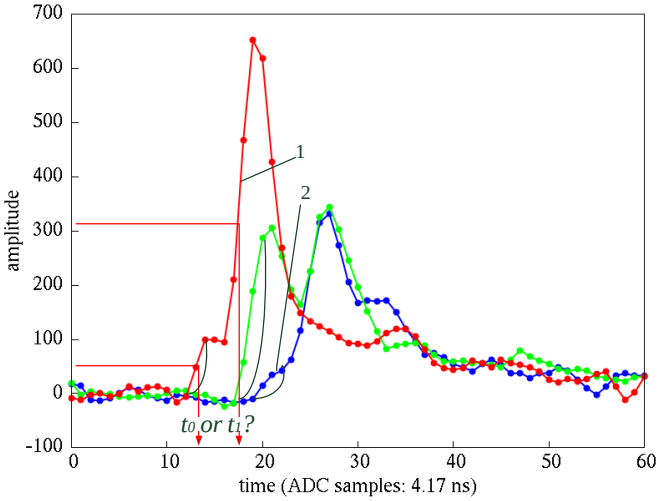

Fig. 9. Sampled responses of 4 straws showing that only a few points on the leading edge are taken into consideration.

One can also observe a dispersion in the arrival of the last clusters due to a spread of primary ionization clusters on the track. The position of the last maximum is not the same (Fig. 10). However, the trailing edge slopes cross in a narrow region, as shown by short straight lines in Fig. 10, which allows us to establish the precise boundary for the arrival time of the very last cluster (wall time).

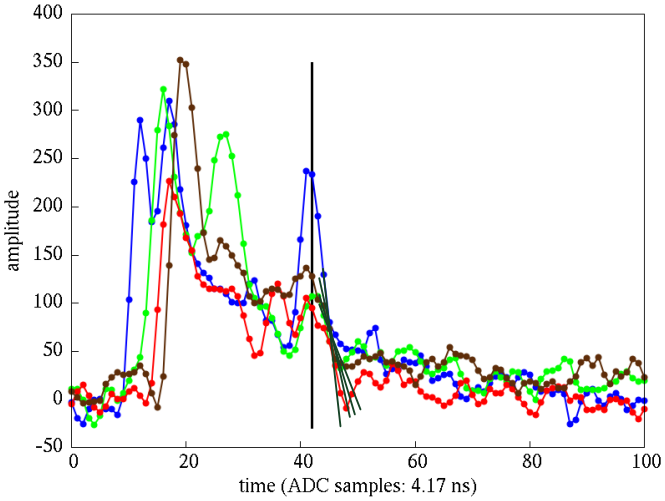

Fig. 10. Sampled responses of a track near the wire. The vertical line indicates the mean position of the last maximum, while the short straight lines show the linear interpolation of the trailing edges. The trailing edge slopes cross in a small region. The last maximum position is not the same.

C. Particle tracks far from the wire

The pulse shape when particles pass far from the wire is similar to the ^{55}Fe response (Fig. 2, Fig. 11). Indeed, the same result can also be obtained by applying the superposition of 2-10 ^{55}Fe pulses arriving at the wire at nearly the same time.

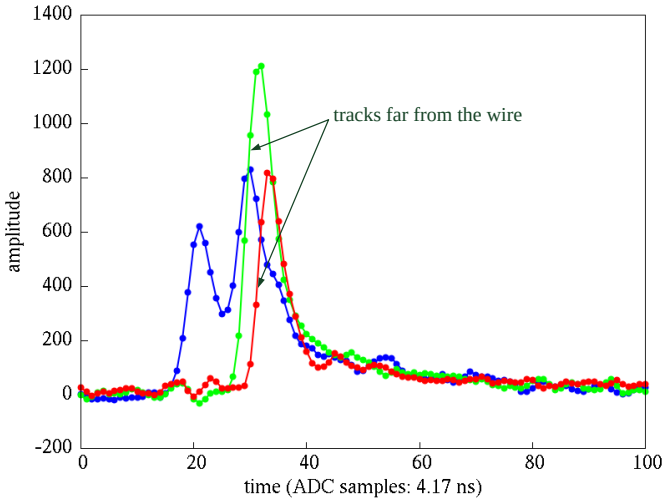

Fig. 11. Sampled responses of the track near the wire and far from the wire.

A track passing 0.3 mm from the tube wall will generate on average 10 primary clusters. This is based on an average spacing of 0.3 mm between primary clusters and a tube diameter of 10 mm. Assuming a drift velocity to be 50 μm/ns, these 10 clusters will arrive at the wire within 6 ns. Taking into account that the leading edge duration of a single cluster is ~8 ns on average, we obtain a regular pulse shape. There are three advantageous properties of this pulse. First off, the peak time of this superposition has to be the same as the peak time of the very last native cluster (if it is considered as not overlapped with other clusters). Therefore, it provides the best reference to the wall time, which is needed for tracking. Furthermore, due to the small spread in the arrival time of the clusters, the leading edge of the summed response provides a well-defined time to calculate the track-to-wire distance. Lastly, the regular pulse shape allows a more accurate fitting, thereby improving the resolution (see Section III).

Since the spread in the arrival times of primary ionization clusters is larger for tracks crossing the tube closer to the wire, the time values from the tracks passing farther from the wire should be assigned a higher weight during the track reconstruction.

The precision of the wall time determination based on single straw data is limited due to the limited statistics of the ionization clusters. It has been improved by including the data of all straws assigned to the track into the analysis. The pulse peak time for particles passing far from the wire combined with the trailing edge times of all straw tube responses belonging to the same track are taken into consideration.

IV. DATA PROCESSING INCLUDING DATA FROM THE NEIGHBORING STRAW TUBES

Here we introduce the signal processing method, including data from the neighboring straws. The purpose is to:

- increase the accuracy and efficiency of the system,
- move much of the computational effort from the offline system to the real-time system running with FPGAs. This is because the clustering operation with the data captured at the rate of 20 GBytes/s becomes the critical path of the offline processing.

A. Event building

When the signal magnitude exceeds a threshold value, then this signal is proposed to be a particle response. Its pulse shape parameters are of interest and have been kept during the event evaluation time. As the trailing edge time is the same for all straw tube signals on the track, the difference in their leading edge times can access the maximum possible drift time value. This value is about 200 ns for our setup. It makes the most significant contribution to the event evaluation time. In addition, the cluster spread, particle propagation time through the straw tubes, and signal delays in the electronic chains must be taken into account.

During the evaluation time the decision about the contribution of this event to the track reconstruction and its weighting has been made.

B. Event filtering

As estimated in Section III, the noise level in the system is comparable to the average single cluster response induced by the proton beam. Therefore, the noise is a very strong factor limiting the system resolution. Below we demonstrate that by comparing neighboring straw signals in real time, we are able to extract a low signal despite the relatively high noise.

First off, the noise fraction has been rejected in real time, reducing the amount of data delivered to the back-end system for offline processing. For this purpose, for each event in the evaluation state (shown for cell 1 in Fig.12), we check the coincidence (event presence) in the neighboring (2) and in the second-order (3) neighboring cells. If no event was measured in the neighboring cells, the event is discarded as noise. If the events in the neighboring cells have the same trailing edge and leading edge parameters (Fig. 13), the event is discarded as electromagnetic disturbance.

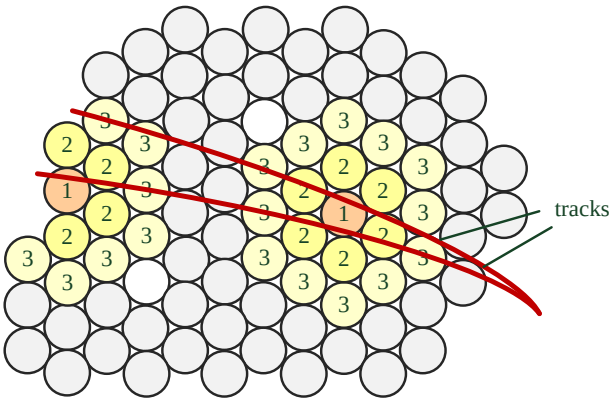

Fig. 12. Event filtering. If an event takes place in cell 1, the event presence in the neighboring cells denoted by 2 and 3 will be checked.

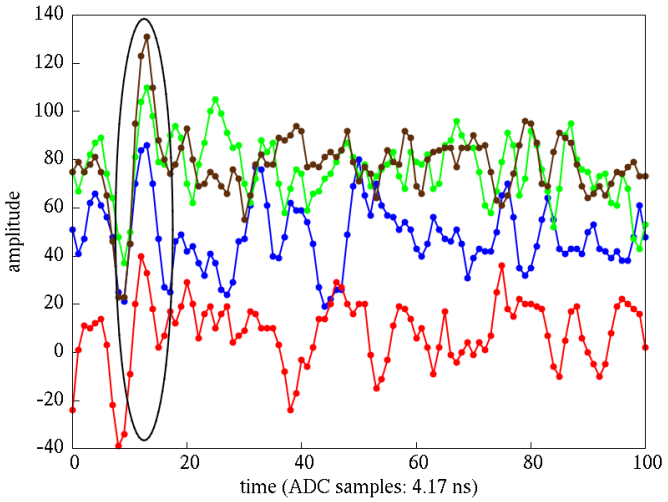

Fig. 13. Electromagnetic pick-up noise.

On the other hand, by analyzing a single track, it becomes possible to process signals close to the noise level. This increases the efficiency of the STT and is especially important for tracks near the wire, which have a low amplitude response. For example, curve 1 in Fig. 14 shows a low amplitude signal. If a coincidence in neighboring channels (curves 2 and 3) is found, it can be processed as a signal generated by a particle.

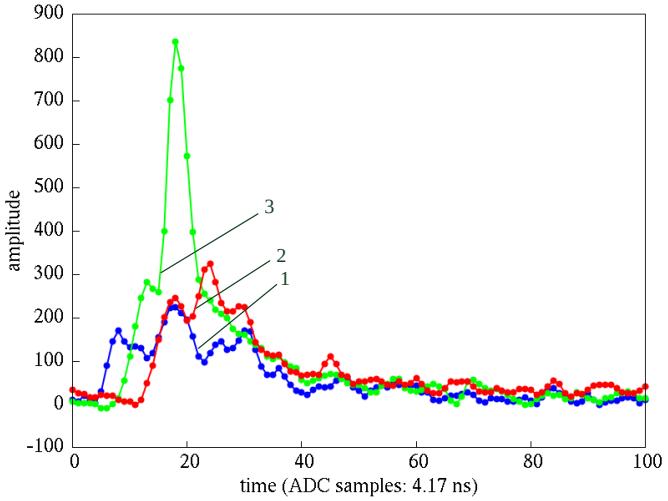

Fig. 14. Low amplitude signal interpretation.

C. *Self-triggering and clustering*

The drift time measurement for the track reconstruction requires a time reference, which is usually provided by a separate scintillator trigger system. It is not necessary in the system presented here, because both leading and trailing edges of the signals have been registered. The trailing edges of all straw tube signals on the track build this time reference. To identify whether the signal belongs to the track, a coincidence search window according to the cluster spread, particle propagation time through the straw tubes, and signal delays in the electronic chains has been established. If the events have their wall time inside this search window, then they have been considered as belonging to the same track and clustered for the track reconstruction. If the number of straws associated with the track is not sufficient for a successful track reconstruction, the events should be discarded. This is another kind of filtering which also reduces the output data stream.

With the clustering, a common wall time is calculated from trailing edge times of all tracks belonging to a cluster. Therefore, this parameter has to be given only once per track.

The amount of data transferred to the back-end system for offline processing depends on the total number of straw tubes, the number of straw tube layers, the maximum drift time and the bin width of calculated times. Considering the specific parameters of the PANDA STT, it has been estimated that clustering results in a data stream reduction of at least 25%.

D. *Multiple track resolution*

The expected total drift time in the PANDA STT is about 100 ns for a fast gas and up to 150 ns for a slow gas. In addition, the shaping time of 8 ns increases the pulse response duration by 40-60 ns. The presence of a magnetic field leads to further pulse expansion up to 300 ns. Thus, within 100-300 ns we cannot distinguish responses to multiple particle tracks based only on single straw tube response.

Track overlap (pile-up) in the STT results in a significant complication of the trigger logic and pattern recognition algorithm. It is estimated, that the event mixing will be about 10% in the PANDA experiment for the innermost layer [1].

Fig. 15 illustrates that by utilizing the neighboring straw data, we can resolve multiple tracks crossing the straw tube at about the same time. The first trailing edge is the same for both pulses, which means that particle 1 crosses both straw tubes. The second particle crosses only one of these tubes. For a sufficient track resolution, the responses of all neighboring straw tubes should be involved.

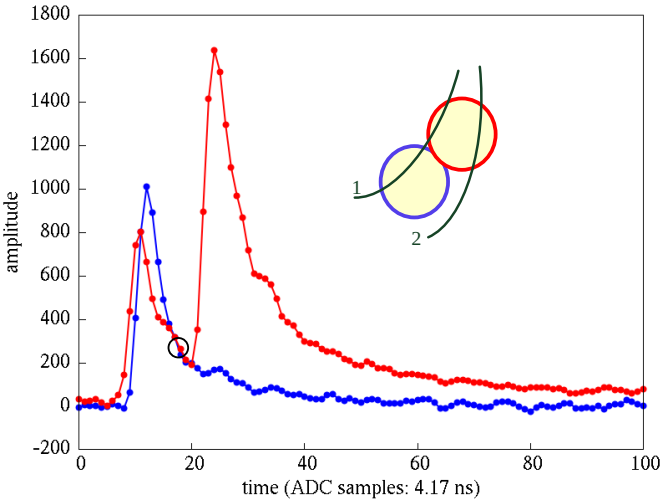

Fig. 15. Double track resolution. Signal pile-up leading to incorrect time measurements.

V. Conclusion

ADC-based signal processing, which is used for data acquisition in the PANDA STT experiment has been investigated. We show clear advantages of the pulse shape

analysis method being applied to the introduced real-time processing including neighboring straw tube data.

In particular, the pulse peak time for straw tubes in which the track passes far from the wire combined with the trailing edge times establish the time reference for tracking – so-called wall time. Thus we select the events belonging to the same track (perform clustering operation) and reduce the data amount delivered to the back-end system by at least 25%. In addition, the offline sorting, which is the most critical path at a high data rate of 20 GByte/s, is eliminated and no external trigger is required.

A detailed analysis of the leading edge allows the position resolution to be improved by selecting information from the very first primary ionization cluster to arrive at the wire. Weighting the results depending upon the track-to-wire distance and noise rejection are the next most important factors to improve the resolution.

The STT efficiency is also significantly improved by being able to process signals close to the noise level and by resolving multiple tracks.

On the other hand, for such a large-scale system, it is very important to reduce the hardware effort without a significant loss of precision. We have showed that reducing the sampling rate down to 120 MHz is possible by increasing the shaping time up to ~20 ns. The latter is still sufficient to obtain all pulse parameters with a very small deviation of ~300 ps compared with the reference 240 MHz setup. Furthermore, with the lowered sample rate, a higher hardware integration level is achieved, which facilitates the implementation of the real-time processing including neighboring straw tube data.

ACKNOWLEDGMENT

We are grateful to our colleague Sergey Furletov for helpful discussions and suggestions.

REFERENCES

[1] PANDA Collaboration, Straw Tube Tracker Technical Design Report, *http://arxiv.org/abs/1205.5441v2*.

[2] WASA Collaboration, Proposal for the Wide Angle Shower Apparatus (WASA) at COSY-Juelich - "WASA at COSY", *http://arxiv.org/abs/nucl-ex/0411038.*

[3] P. Kulessa et al., A sampling ADC as a universal tool for data processing and trigger application, Proceedings of Science, http://pos.sissa.it//archive/conferences/160/012/Bormio2012_012.pdf.

[4] H. Fischle, J. Heintze, and B. Schmidt, "Experimental determination of ionization cluster size distributions in counting gases," *Nuclear instruments and methods in physics research*, section A301, pp. 202-214, 1991.

[5] F. Sauli, "Principles of operation of multiwire proportional and drift chambers," Lectures given in the Academic Training Programme of CERN, 1977, *http://pdg.lbl.gov/*.

[6] T. Akesson et al., "Particle identification using the Time-over-threshold method in the ATLAS Transition Radiation Tracker," *Nuclear instruments and methods in physics research*, section A474, pp. 172-187, 2001.

[7] E. Abat et al., "The ATLAS TRT Electronics," JINST 3 P06007, 2008.

[8] P. Hansen, Lecture on gaseous tracking detectors, *http://www.nbi.dk/~phansen/experimental/week10/tracking.pdf*

[9] R. Maier, "Cooler synchrotron COSY — Performance and perspectives," *Nuclear instruments and methods in physics research*, section A390, pp. 1-8, 1997.